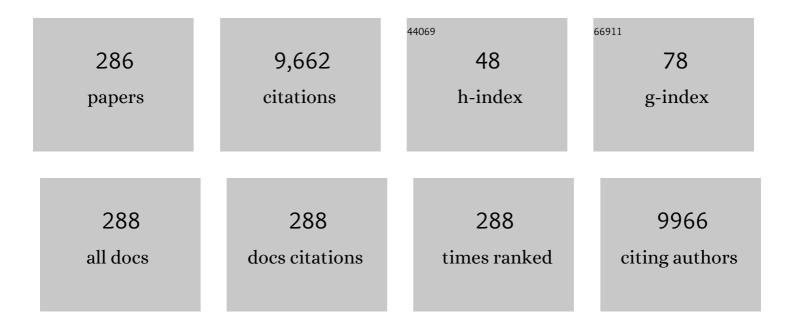
Nageh Allam

List of Publications by Year in descending order

Source: https://exaly.com/author-pdf/2135266/publications.pdf Version: 2024-02-01



#	Article	IF	CITATIONS
1	Recent Advances in the Use of TiO ₂ Nanotube and Nanowire Arrays for Oxidative Photoelectrochemistry. Journal of Physical Chemistry C, 2009, 113, 6327-6359.	3.1	776
2	Photoelectrochemical and water photoelectrolysis properties of ordered TiO2 nanotubes fabricated by Ti anodization in fluoride-free HCl electrolytes. Journal of Materials Chemistry, 2008, 18, 2341.	6.7	198
3	Co–Cu Bimetallic Metal Organic Framework Catalyst Outperforms the Pt/C Benchmark for Oxygen Reduction. Journal of the American Chemical Society, 2021, 143, 4064-4073.	13.7	175
4	Impact of nanotechnology on biogas production: A mini-review. Renewable and Sustainable Energy Reviews, 2015, 50, 1392-1404.	16.4	144
5	Impact of Nanotechnology on Enhanced Oil Recovery: A Mini-Review. Industrial & Engineering Chemistry Research, 2019, 58, 16287-16295.	3.7	133
6	Formation of Vertically Oriented TiO ₂ Nanotube Arrays using a Fluoride Free HCl Aqueous Electrolyte. Journal of Physical Chemistry C, 2007, 111, 13028-13032.	3.1	132
7	A facile electrosynthesis approach of amorphous Mn-Co-Fe ternary hydroxides as binder-free active electrode materials for high-performance supercapacitors. Electrochimica Acta, 2019, 296, 59-68.	5.2	128
8	Self-Assembled Fabrication of Vertically Oriented Ta ₂ O ₅ Nanotube Arrays, and Membranes Thereof, by One-Step Tantalum Anodization. Chemistry of Materials, 2008, 20, 6477-6481.	6.7	121
9	TiO ₂ Nanotube/CdS Hybrid Electrodes: Extraordinary Enhancement in the Inactivation of <i>Escherichia coli</i> . Journal of the American Chemical Society, 2010, 132, 14406-14408.	13.7	121
10	A review of the effects of benzotriazole on the corrosion of copper and copper alloys in clean and polluted environments. Journal of Applied Electrochemistry, 2009, 39, 961-969.	2.9	119
11	3D Interconnected Binder-Free Electrospun MnO@C Nanofibers for Supercapacitor Devices. Scientific Reports, 2018, 8, 7988.	3.3	113
12	Thermodynamic and quantum chemistry characterization of the adsorption of triazole derivatives during Muntz corrosion in acidic and neutral solutions. Applied Surface Science, 2007, 253, 4570-4577.	6.1	106
13	Recent advances in the design of cathode materials for Li-ion batteries. RSC Advances, 2020, 10, 21662-21685.	3.6	106
14	A General Method for the Anodic Formation of Crystalline Metal Oxide Nanotube Arrays without the Use of Thermal Annealing. Advanced Materials, 2008, 20, 3942-3946.	21.0	104
15	Asymmetric supercapacitors based on 3D graphene-wrapped V2O5 nanospheres and Fe3O4@3D graphene electrodes with high power and energy densities. Electrochimica Acta, 2019, 310, 58-69.	5.2	99
16	Nanostructured spinel manganese cobalt ferrite for high-performance supercapacitors. RSC Advances, 2017, 7, 51888-51895.	3.6	98
17	Semi-transparent perovskite solar cells: unveiling the trade-off between transparency and efficiency. Journal of Materials Chemistry A, 2018, 6, 19696-19702.	10.3	95
18	Effect of cathode material on the morphology and photoelectrochemical properties of vertically oriented TiO2 nanotube arrays. Solar Energy Materials and Solar Cells, 2008, 92, 1468-1475.	6.2	93

#	Article	IF	CITATIONS
19	Bacteriorhodopsin/TiO2 nanotube arrays hybrid system for enhanced photoelectrochemical water splitting. Energy and Environmental Science, 2011, 4, 2909.	30.8	93
20	Photoelectrochemical Water Oxidation Characteristics of Anodically Fabricated TiO ₂ Nanotube Arrays: Structural and Optical Properties. Journal of Physical Chemistry C, 2010, 114, 12024-12029.	3.1	91
21	Electrochemical fabrication of complex copper oxide nanoarchitectures via copper anodization in aqueous and non-aqueous electrolytes. Materials Letters, 2011, 65, 1949-1955.	2.6	91
22	Room Temperature One-Step Polyol Synthesis of Anatase TiO ₂ Nanotube Arrays: Photoelectrochemical Properties. Langmuir, 2009, 25, 7234-7240.	3.5	89
23	Electrochemical Fabrication of Strontium-Doped TiO ₂ Nanotube Array Electrodes and Investigation of Their Photoelectrochemical Properties. Journal of Physical Chemistry C, 2011, 115, 13480-13486.	3.1	88
24	Three-Dimensional Interconnected Binder-Free Mn–Ni–S Nanosheets for High Performance Asymmetric Supercapacitor Devices with Exceptional Cyclic Stability. ACS Applied Energy Materials, 2019, 2, 3717-3725.	5.1	88
25	Enhanced Photoassisted Water Electrolysis Using Vertically Oriented Anodically Fabricated Tiâ^'Nbâ^'Zrâ^'O Mixed Oxide Nanotube Arrays. ACS Nano, 2010, 4, 5819-5826.	14.6	85
26	Untapped Potential of Polymorph MoS ₂ : Tuned Cationic Intercalation for High-Performance Symmetric Supercapacitors. ACS Applied Materials & Interfaces, 2019, 11, 33955-33965.	8.0	80
27	TiO2 nanoparticles optimized for photoanodes tested in large area Dye-sensitized solar cells (DSSC). Solar Energy Materials and Solar Cells, 2016, 153, 108-116.	6.2	77
28	Vertically Oriented Ti–Pd Mixed Oxynitride Nanotube Arrays for Enhanced Photoelectrochemical Water Splitting. ACS Nano, 2011, 5, 5056-5066.	14.6	76
29	Unveiling the Effect of the Structure of Carbon Material on the Charge Storage Mechanism in MoS ₂ -Based Supercapacitors. ACS Omega, 2018, 3, 16301-16308.	3.5	76
30	Recent advances in the use of TiO ₂ nanotube powder in biological, environmental, and energy applications. Nanoscale Advances, 2019, 1, 2801-2816.	4.6	73
31	Adenine-functionalized Spongy Graphene for Green and High-Performance Supercapacitors. Scientific Reports, 2017, 7, 43104.	3.3	71
32	N-doped carbon quantum dots boost the electrochemical supercapacitive performance and cyclic stability of MoS2. Journal of Energy Storage, 2020, 27, 101078.	8.1	69
33	Mesoporous spinel manganese zinc ferrite for high-performance supercapacitors. Journal of Electroanalytical Chemistry, 2018, 817, 111-117.	3.8	67
34	Low power UV photodetection characteristics of cross-linked ZnO nanorods/nanotetrapods grown on silicon chip. Sensors and Actuators A: Physical, 2013, 192, 124-129.	4.1	64
35	Electrospun Mesoporous Mn–V–O@C Nanofibers for High-Performance Asymmetric Supercapacitor Devices with High Stability. ACS Sustainable Chemistry and Engineering, 2019, 7, 13471-13480.	6.7	64
36	Eco-friendly facile synthesis of glucose–derived microporous carbon spheres electrodes with enhanced performance for water capacitive deionization. Desalination, 2020, 477, 114278.	8.2	63

#	Article	IF	CITATIONS
37	Novel MWCNTs/graphene oxide/pyrogallol composite with enhanced sensitivity for biosensing applications. Biosensors and Bioelectronics, 2017, 89, 1034-1041.	10.1	60
38	3D spongy graphene-modified screen-printed sensors for the voltammetric determination of the narcotic drug codeine. Biosensors and Bioelectronics, 2018, 101, 90-95.	10.1	58
39	Novel Z-Scheme/Type-II CdS@ZnO/g-C3N4 ternary nanocomposites for the durable photodegradation of organics: Kinetic and mechanistic insights. Chemosphere, 2021, 277, 128730.	8.2	58
40	Functionalized cellulose-magnetite nanocomposite catalysts for efficient biodiesel production. Chemical Engineering Journal, 2017, 322, 167-180.	12.7	56
41	Unveiling CO adsorption on Cu surfaces: new insights from molecular orbital principles. Physical Chemistry Chemical Physics, 2018, 20, 25892-25900.	2.8	56
42	Unravelling the interplay of crystal structure and electronic band structure of tantalum oxide (Ta ₂ O ₅). Physical Chemistry Chemical Physics, 2013, 15, 1352-1357.	2.8	55
43	Interface Architecture Determined Electrocatalytic Activity of Pt on Vertically Oriented TiO ₂ Nanotubes. ACS Applied Materials & Interfaces, 2011, 3, 147-151.	8.0	53
44	Towards nanostructured perovskite solar cells with enhanced efficiency: Coupled optical and electrical modeling. Solar Energy, 2016, 137, 364-370.	6.1	53
45	Rational design of porous binary Pt-based nanodendrites as efficient catalysts for direct glucose fuel cells over a wide pH range. Catalysis Science and Technology, 2017, 7, 2819-2827.	4.1	53
46	Effect of Rapid Infrared Annealing on the Photoelectrochemical Properties of Anodically Fabricated TiO2 Nanotube Arrays. Journal of Physical Chemistry C, 2009, 113, 7996-7999.	3.1	52
47	Morphological and structural characterization of single-crystal ZnO nanorod arrays on flexible and non-flexible substrates. Beilstein Journal of Nanotechnology, 2015, 6, 720-725.	2.8	52
48	Bimetallic Co–W–S Chalcogenides Confined in N,S-Codoped Porous Carbon Matrix Derived from Metal–Organic Frameworks for Highly Stable Electrochemical Supercapacitors. ACS Applied Energy Materials, 2020, 3, 8064-8074.	5.1	52
49	Facile Synthesis of Nanostructured Binary Ni–Cu Phosphides as Advanced Battery Materials for Asymmetric Electrochemical Supercapacitors. ACS Applied Energy Materials, 2020, 3, 9305-9314.	5.1	52
50	TiO ₂ nanotubes with ultrathin walls for enhanced water splitting. Chemical Communications, 2015, 51, 12617-12620.	4.1	50
51	An Experimental Insight into the Structural and Electronic Characteristics of Strontiumâ€Doped Titanium Dioxide Nanotube Arrays. Advanced Functional Materials, 2014, 24, 6783-6796.	14.9	49
52	Vertically aligned crystalline silicon nanowires with controlled diameters for energy conversion applications: Experimental and theoretical insights. Journal of Applied Physics, 2014, 115, .	2.5	48
53	TiO ₂ Nanotube-Based Dye-Sensitized Solar Cell Using New Photosensitizer with Enhanced Open-Circuit Voltage and Fill Factor. ACS Applied Materials & Interfaces, 2012, 4, 4413-4418.	8.0	47
54	Thermal/Electrochemical Growth and Characterization of One-Dimensional ZnO/TiO ₂ Hybrid Nanoelectrodes for Solar Fuel Production. Journal of Physical Chemistry C, 2013, 117, 18502-18509.	3.1	47

#	Article	IF	CITATIONS
55	Recent advances in the use of metal oxide-based photocathodes for solar fuel production. Journal of Renewable and Sustainable Energy, 2014, 6, .	2.0	47
56	A facile electrosynthesis approach of Mn-Ni-Co ternary phosphides as binder-free active electrode materials for high-performance electrochemical supercapacitors. Electrochimica Acta, 2021, 380, 138197.	5.2	47
57	Unveiling the Synergistic Effect of ZnO Nanoparticles and Surfactant Colloids for Enhanced Oil Recovery. Colloids and Interface Science Communications, 2019, 29, 33-39.	4.1	46
58	Novel Bi-based photocatalysts with unprecedented visible light-driven hydrogen production rate: Experimental and DFT insights. Chemical Engineering Journal, 2020, 384, 123351.	12.7	46
59	Metal–Organic frameworks encapsulated with vanadium-substituted heteropoly acid for highly stable asymmetric supercapacitors. Journal of Energy Storage, 2020, 28, 101292.	8.1	46
60	Growth of vertically aligned ZnO nanorods on Teflon as a novel substrate for low-power flexible light sensors. Applied Physics A: Materials Science and Processing, 2015, 119, 1197-1201.	2.3	45
61	Wind energy systems: Analysis of the self-starting physics of vertical axis wind turbine. Renewable and Sustainable Energy Reviews, 2018, 81, 1602-1610.	16.4	45
62	Hybrid supercapacitors: A simple electrochemical approach to determine optimum potential window and charge balance. Journal of Power Sources, 2020, 480, 229152.	7.8	45
63	Morphology–photoactivity relationship: WO 3 nanostructured films for solar hydrogen production. International Journal of Hydrogen Energy, 2016, 41, 866-872.	7.1	44
64	Enhanced photoelectrochemical water splitting characteristics of TiO2 hollow porous spheres by embedding graphene as an electron transfer channel. International Journal of Hydrogen Energy, 2017, 42, 29131-29139.	7.1	44
65	Effects of benzotriazole on the corrosion of Cu10Ni alloy in sulfide-polluted salt water. Corrosion Science, 2005, 47, 2280-2292.	6.6	43
66	Wide visible emission and narrowing band gap in Cd-doped ZnO nanopowders synthesized via sol-gel route. Journal of Alloys and Compounds, 2016, 687, 920-926.	5.5	43
67	Photoelectrochemical water splitting by defects in nanostructured multinary transition metal oxides. Solar Energy Materials and Solar Cells, 2019, 194, 184-194.	6.2	43
68	Stable solar-driven water splitting by anodic ZnO nanotubular semiconducting photoanodes. RSC Advances, 2016, 6, 80221-80225.	3.6	42
69	One-step, calcination-free synthesis of zinc cobaltite nanospheres for high-performance supercapacitors. Materials Today Energy, 2017, 4, 97-104.	4.7	41
70	Non-precious co-catalysts boost the performance ofÂTiO2 hierarchical hollow mesoporous spheres inÂsolar fuel cells. International Journal of Hydrogen Energy, 2018, 43, 21219-21230.	7.1	41
71	Recycling of Liâ ``Niâ ``Mnâ ``Co Hydroxide from Spent Batteries to Produce Highâ€Performance Supercapacitors with Exceptional Stability. ChemElectroChem, 2020, 7, 975-982.	3.4	41
72	On the nature of defect states in tungstate nanoflake arrays as promising photoanodes in solar fuel cells. Physical Chemistry Chemical Physics, 2016, 18, 22217-22223.	2.8	40

#	Article	IF	CITATIONS
73	Silver Nanoparticles-Decorated Titanium Oxynitride Nanotube Arrays for Enhanced Solar Fuel Generation. Scientific Reports, 2017, 7, 1913.	3.3	40
74	Cost-Effective Face Mask Filter Based on Hybrid Composite Nanofibrous Layers with High Filtration Efficiency. Langmuir, 2021, 37, 7492-7502.	3.5	40
75	ZnO nano-tetrapod photoanodes for enhanced solar-driven water splitting. Chemical Physics Letters, 2012, 549, 62-66.	2.6	39
76	A first-principles roadmap and limits to design efficient supercapacitor electrode materials. Physical Chemistry Chemical Physics, 2019, 21, 17494-17511.	2.8	39
77	Recent advances on zeolitic imidazolate -67 metal-organic framework-derived electrode materials for electrochemical supercapacitors. Journal of Energy Storage, 2021, 34, 102195.	8.1	39
78	Effect of cysteine on the electrochemical behavior of Cu10Ni alloy in sulfide polluted environments: Experimental and theoretical aspects. Materials Chemistry and Physics, 2012, 136, 1-9.	4.0	38
79	Layered Tantalum Oxynitride Nanorod Array Carpets for Efficient Photoelectrochemical Conversion of Solar Energy: Experimental and DFT Insights. ACS Applied Materials & Interfaces, 2014, 6, 4609-4615.	8.0	38
80	Microwave-assisted chemical bath deposition of nanocrystalline CdS thin films with superior photodetection characteristics. Sensors and Actuators A: Physical, 2015, 230, 9-16.	4.1	38
81	Nanostructured tantala as a template for enhanced osseointegration. Nanotechnology, 2009, 20, 045102.	2.6	37
82	The DFT+U: Approaches, Accuracy, and Applications. , 0, , .		37
83	Tin–zinc-oxide nanocomposites (SZO) as promising electron transport layers for efficient and stable perovskite solar cells. Nanoscale Advances, 2019, 1, 2654-2662.	4.6	37
84	Nanocrystalline Cellulose Confined in Amorphous Carbon Fibers as Capacitor Material for Efficient Energy Storage. Journal of Physical Chemistry C, 2020, 124, 7007-7015.	3.1	37
85	Effect of Ni-Ferrite and Ni-Co-Ferrite nanostructures on biogas production from anaerobic digestion. Fuel, 2019, 254, 115673.	6.4	36
86	Ge-doped ZnO nanorods grown on FTO for photoelectrochemical water splitting with exceptional photoconversion efficiency. International Journal of Hydrogen Energy, 2021, 46, 209-220.	7.1	36
87	Nanostructuring for enhanced absorption and carrier collection in CZTS-based solar cells: Coupled optical and electrical modeling. Optical Materials, 2016, 54, 84-88.	3.6	35
88	Self-assembled growth of vertically aligned ZnO nanorods for light sensing applications. Materials Letters, 2014, 137, 45-48.	2.6	34
89	Recent Advances in the Regenerative Approaches for Traumatic Spinal Cord Injury: Materials Perspective. ACS Biomaterials Science and Engineering, 2020, 6, 6490-6509.	5.2	34

#	Article	IF	CITATIONS
91	Computational study on oxynitride perovskites for CO2 photoreduction. Energy Conversion and Management, 2016, 122, 207-214.	9.2	33
92	Tuning The Photoactivity of Zirconia Nanotubes-Based Photoanodes via Ultrathin Layers of ZrN: An Effective Approach toward Visible-Light Water Splitting. Journal of Physical Chemistry C, 2016, 120, 7025-7032.	3.1	33
93	Efficient fabrication methodology of wide angle black silicon for energy harvesting applications. RSC Advances, 2017, 7, 26974-26982.	3.6	33
94	Recent advances on electrospun scaffolds as matrices for tissue-engineered heart valves. Materials Today Chemistry, 2017, 5, 11-23.	3.5	33
95	Robust photoactive nanoadsorbents with antibacterial activity for the removal of dyes. Journal of Hazardous Materials, 2019, 378, 120679.	12.4	33
96	ZnO nanorods/polyaniline heterojunctions for low-power flexible light sensors. Materials Chemistry and Physics, 2016, 181, 7-11.	4.0	32
97	CoFe ₂ O ₄ @Carbon Spheres Electrode: A One‣tep Solvothermal Method for Enhancing the Electrochemical Performance of Hybrid Supercapacitors. ChemElectroChem, 2020, 7, 526-534.	3.4	32
98	Bioactive and Elastic Nanocomposites with Antimicrobial Properties for Bone Tissue Regeneration. ACS Applied Bio Materials, 2020, 3, 3313-3325.	4.6	32
99	Biocompatible PCL-nanofibers scaffold with immobilized fibronectin and laminin for neuronal tissue regeneration. Materials Science and Engineering C, 2021, 119, 111550.	7.3	32
100	Superior visible light antimicrobial performance of facet engineered cobalt doped TiO2 mesocrystals in pathogenic bacterium and fungi. Scientific Reports, 2021, 11, 5609.	3.3	32
101	Binder-Free Electrospun Ni–Mn–O Nanofibers Embedded in Carbon Shells with Ultrahigh Energy and Power Densities for Highly Stable Next-Generation Energy Storage Devices. Langmuir, 2021, 37, 5161-5171.	3.5	32
102	Unveiling the Optimal Interfacial Synergy of Plasmaâ€Modulated Trimetallic Mnâ€Niâ€Co Phosphides: Tailoring Deposition Ratio for Complementary Water Splitting. Energy and Environmental Materials, 2023, 6, .	12.8	32
103	Self-Standing Crystalline TiO2Nanotubes/CNTs Heterojunction Membrane: Synthesis and Characterization. ACS Applied Materials & amp; Interfaces, 2011, 3, 952-955.	8.0	31
104	Graphene Quantum Sheets with Multiband Emission: Unravelling the Molecular Origin of Graphene Quantum Dots. Journal of Physical Chemistry C, 2016, 120, 21678-21684.	3.1	31
105	Ultrahigh performance of novel energy-efficient capacitive deionization electrodes based on 3D nanotubular composites. New Journal of Chemistry, 2018, 42, 3560-3567.	2.8	31
106	High-performance solid-state supercapacitor based on Ni-Co layered double hydroxide@Co3O4 nanocubes and spongy graphene electrodes. Applied Surface Science, 2022, 587, 152548.	6.1	31
107	Self-assembled zirconia nanotube arrays: fabrication mechanism, energy consideration and optical activity. RSC Advances, 2014, 4, 36336-36343.	3.6	30
108	In Situ Formation of Graphene Stabilizes Zero-Valent Copper Nanoparticles and Significantly Enhances the Efficiency of Photocatalytic Water Splitting. ACS Sustainable Chemistry and Engineering, 2018, 6, 16876-16885.	6.7	30

#	Article	IF	CITATIONS
109	Supercapattery electrode materials by Design: Plasma-induced defect engineering of bimetallic oxyphosphides for energy storage. Journal of Colloid and Interface Science, 2021, 603, 478-490.	9.4	30
110	Effect of complexing agents on the electrodeposition of Cu–Zn–Sn metal precursors and corresponding Cu2ZnSnS4-based solar cells. Journal of Electroanalytical Chemistry, 2014, 735, 129-135.	3.8	29
111	Novel mineralized electrospun chitosan/PVA/TiO ₂ nanofibrous composites for potential biomedical applications: computational and experimental insights. Nanoscale Advances, 2020, 2, 1512-1522.	4.6	29
112	Innovative nanocomposite formulations for enhancing biogas and biofertilizers production from anaerobic digestion of organic waste. Bioresource Technology, 2020, 309, 123350.	9.6	29
113	Fullerene C ₇₆ : An Unexplored Superior Electrode Material with Wide Operating Potential Window for Highâ€Performance Supercapacitors. ChemElectroChem, 2020, 7, 1672-1678.	3.4	28
114	Unravelling the correlated electronic and optical properties of BaTaO ₂ N with perovskite-type structure as a potential candidate for solar energy conversion. Physical Chemistry Chemical Physics, 2014, 16, 18418-18424.	2.8	27
115	10-fold enhancement in light-driven water splitting using niobium oxynitride microcone array films. Solar Energy Materials and Solar Cells, 2016, 151, 149-153.	6.2	27
116	DFT insights into the electronic properties and adsorption of NO ₂ on metal-doped carbon nanotubes for gas sensing applications. New Journal of Chemistry, 2017, 41, 14936-14944.	2.8	27
117	A Study of Low-Temperature CO Oxidation over Mesoporous CuO-TiO2 Nanotube Catalysts. Catalysts, 2017, 7, 129.	3.5	27
118	Propping the optical and electronic properties of potential photo-sensitizers with different ï€-spacers: TD-DFT insights. Spectrochimica Acta - Part A: Molecular and Biomolecular Spectroscopy, 2018, 188, 237-243.	3.9	27
119	Eco-friendly, one-step synthesis of cobalt sulfide-decorated functionalized graphene for high-performance supercapacitors. Journal of Energy Storage, 2019, 24, 100760.	8.1	27
120	Transition Metal Selenide (TMSe) electrodes for electrochemical capacitor devices: A critical review. Journal of Energy Storage, 2022, 47, 103565.	8.1	27
121	Interface properties determined the performance of thermally grown GaN/Si heterojunction solar cells. Solar Energy, 2013, 98, 485-491.	6.1	26
122	Sub-100 nm TiO2 tubular architectures for efficient solar energy conversion. Journal of Materials Chemistry A, 2016, 4, 9375-9380.	10.3	26
123	Novel design of plasmonic and dielectric antireflection coatings to enhance the efficiency of perovskite solar cells. Solar Energy, 2018, 174, 803-814.	6.1	26
124	Computational Design of Novel Hydrogen-Doped, Oxygen-Deficient Monoclinic Zirconia with Excellent Optical Absorption and Electronic Properties. Scientific Reports, 2019, 9, 10159.	3.3	26
125	Black titania nanotubes/spongy graphene nanocomposites for high-performance supercapacitors. RSC Advances, 2019, 9, 12555-12566.	3.6	26
126	Green, single-pot synthesis of functionalized Na/N/P co-doped graphene nanosheets for high-performance supercapacitors. Journal of Electroanalytical Chemistry, 2019, 837, 30-38.	3.8	26

#	Article	IF	CITATIONS
127	A Catalyst-Free Growth of ZnO Nanowires on Si (100) Substrates: Effect of Substrate Position on Morphological, Structural and Optical Properties. ECS Journal of Solid State Science and Technology, 2012, 1, P86-P89.	1.8	25
128	Heteroepitaxial growth of GaN/Si (111) junctions in ammonia-free atmosphere: Charge transport, optoelectronic, and photovoltaic properties. Journal of Applied Physics, 2013, 113, .	2.5	25
129	Electrical Characterization of Nanopolyaniline/Porous Silicon Heterojunction at High Temperatures. Journal of Nanomaterials, 2013, 2013, 1-8.	2.7	25
130	Electrospun Lead-Free All-Inorganic Double Perovskite Nanofibers for Photovoltaic and Optoelectronic Applications. ACS Applied Nano Materials, 2019, 2, 7085-7094.	5.0	25
131	Niobium–Zirconium Oxynitride Nanotube Arrays for Photoelectrochemical Water Splitting. ACS Applied Nano Materials, 2020, 3, 6078-6088.	5.0	25
132	Improved genistein loading and release on electrospun chitosan nanofiber blends. Journal of Molecular Liquids, 2016, 223, 1056-1061.	4.9	24
133	Refractory plasmonics enabling 20% efficient lead-free perovskite solar cells. Scientific Reports, 2020, 10, 6732.	3.3	24
134	Optimized electrosynthesis approach of Manganese-Nickel- Cobalt chalcogenide nanosheet arrays as binder-free battery materials for asymmetric electrochemical supercapacitors. Electrochimica Acta, 2021, 396, 139191.	5.2	24
135	Effect of Glycine on the Electrochemical and Stress Corrosion Cracking Behavior of Cu10Ni Alloy in Sulfide Polluted Salt Water. Industrial & Engineering Chemistry Research, 2011, 50, 8796-8802.	3.7	23
136	Ternary Ti–Mo–Ni mixed oxide nanotube arrays as photoanode materials for efficient solar hydrogen production. Physical Chemistry Chemical Physics, 2013, 15, 12274.	2.8	23
137	Electrochemical Determination of the Serotonin Reuptake Inhibitor, Dapoxetine, Using Cesium–Gold Nanoparticles. ACS Omega, 2017, 2, 6628-6635.	3.5	23
138	On the relationship between rutile/anatase ratio and the nature of defect states in sub-100 nm TiO ₂ nanostructures: experimental insights. Physical Chemistry Chemical Physics, 2018, 20, 5975-5982.	2.8	23
139	An engineered nanocomposite for sensitive and selective detection of mercury in environmental water samples. Analytical Methods, 2018, 10, 2526-2535.	2.7	23
140	Natural silk for energy and sensing applications: a review. Environmental Chemistry Letters, 2021, 19, 2141-2155.	16.2	23
141	Promoting effect of low concentration of benzotriazole on the corrosion of Cu10Ni alloy in sulfide polluted salt water. Applied Surface Science, 2008, 254, 5007-5011.	6.1	22
142	Effect of alloying elements on the electrochemical behavior of Cu–Ni–Zn ternary system in sulfide-polluted saltwater. Applied Surface Science, 2014, 307, 621-630.	6.1	22
143	Unravelling the interplay of dopant concentration and band structure engineering of monoclinic niobium pentoxide: AÂmodelÂphotoanode for water splitting. International Journal of Hydrogen Energy, 2015, 40, 13867-13875.	7.1	22
144	Smart bi-metallic perovskite nanofibers as selective and reusable sensors of nano-level concentrations of non-steroidal anti-inflammatory drugs. Talanta, 2018, 185, 344-351.	5.5	22

#	Article	IF	CITATIONS
145	Functional Nanoarchitectures For Enhanced Drug Eluting Stents. Scientific Reports, 2017, 7, 40291.	3.3	21
146	From Rusting to Solar Power Plants: A Successful Nano-Pattering of Stainless Steel 316L for Visible Light-Induced Photoelectrocatalytic Water Splitting. ACS Sustainable Chemistry and Engineering, 2018, 6, 17352-17358.	6.7	21
147	Electrochemical nano-patterning of brass for stable and visible light-induced photoelectrochemical water splitting. International Journal of Hydrogen Energy, 2019, 44, 14588-14595.	7.1	21
148	Comparison between Benzothiadizole–Thiophene- and Benzothiadizole–Furan-Based D–Aâ^'π–A Dyes Applied in Dye-Sensitized Solar Cells: Experimental and Theoretical Insights. ACS Omega, 2020, 5, 16856-16864.	3.5	21
149	Microbial fuel cells with enhanced bacterial catalytic activity and stability using 3D nanoporous stainless steel anode. Journal of Cleaner Production, 2021, 285, 124816.	9.3	21
150	Influence of precursor thin films stacking order on the properties of Cu2ZnSnS4 thin films fabricated by electrochemical deposition method. Superlattices and Microstructures, 2014, 76, 339-348.	3.1	20
151	Self-Assembled Nanostructured Photoanodes with Staggered Bandgap for Efficient Solar Energy Conversion. ACS Nano, 2014, 8, 4915-4923.	14.6	20
152	Synthesis and characterization of core–shell structured M@Pd/SnO ₂ –graphene [M = Co, Ni or Cu] electrocatalysts for ethanol oxidation in alkaline solution. New Journal of Chemistry, 2018, 42, 6144-6160.	2.8	20
153	Mineralization of electrospun gelatin/CaCO3 composites: A new approach for dental applications. Materials Science and Engineering C, 2019, 100, 655-664.	7.3	20
154	Facile template-free one-pot room-temperature synthesis of novel m-Bi(OH)CrO4 microspheres. Materials Letters, 2020, 262, 127188.	2.6	20
155	Ultrathin ALD TiO2 shells for enhanced photoelectrochemical solar fuel generation. Journal of Alloys and Compounds, 2018, 739, 178-183.	5.5	19
156	Unbiased spontaneous solar hydrogen production using stable TiO ₂ –CuO composite nanofiber photocatalysts. RSC Advances, 2018, 8, 37219-37228.	3.6	19
157	Enhanced photoelectrochemical water splitting via engineered surface defects of BiPO4 nanorod photoanodes. International Journal of Hydrogen Energy, 2021, 46, 23214-23224.	7.1	19
158	Highly Stable Supercapacitor Devices Based on Three-Dimensional Bioderived Carbon Encapsulated g-C ₃ N ₄ Nanosheets. ACS Applied Energy Materials, 2021, 4, 10344-10355.	5.1	19
159	Facile Surface Treatment of Industrial Stainless Steel Waste Meshes at Mild Conditions to Produce Efficient Oxygen Evolution Catalysts. Energy & Fuels, 2022, 36, 7025-7034.	5.1	19
160	Thermodynamic and efficiency analysis of solar thermochemical water splitting using Ce–Zr mixtures. Solar Energy, 2016, 135, 154-162.	6.1	18
161	Highly active, durable and pH-universal hybrid oxide nanocrystals for efficient oxygen evolution. Sustainable Energy and Fuels, 2017, 1, 1123-1129.	4.9	18
162	Refractory plasmonics boost the performance of thin-film solar cells. Emergent Materials, 2018, 1, 185-191.	5.7	18

#	Article	IF	CITATIONS
163	Genistein Loaded Nanofibers Protect Spinal Cord Tissue Following Experimental Injury in Rats. Biomedicines, 2018, 6, 96.	3.2	18
164	Emerging nanoporous anodized stainless steel for hydrogen production from solar water splitting. Journal of Cleaner Production, 2020, 274, 122826.	9.3	18
165	Recent progress in the development of hole-transport materials to boost the power conversion efficiency of perovskite solar cells. Sustainable Materials and Technologies, 2020, 26, e00210.	3.3	18
166	Multi-walled vanadium oxide nanotubes modified 3D microporous bioderived carbon as novel electrodes for hybrid capacitive deionization. Separation and Purification Technology, 2021, 266, 118597.	7.9	18
167	Controlled fabrication of mesoporous electrodes with unprecedented stability for water capacitive deionization under harsh conditions in large size cells. Desalination, 2021, 511, 115099.	8.2	18
168	Towards Cs-ion supercapacitors: Cs intercalation in polymorph MoS ₂ as a model 2D electrode material. Chemical Communications, 2021, 57, 3231-3234.	4.1	18
169	A mesoporous ternary transition metal oxide nanoparticle composite for high-performance asymmetric supercapacitor devices with high specific energy. Nanoscale Advances, 2022, 4, 1387-1393.	4.6	18
170	Propping the electrochemical impedance spectra at different voltages reveals the untapped supercapacitive performance of materials. Electrochimica Acta, 2022, 408, 139932.	5.2	18
171	Solvent solution-dependent properties of nonstoichiometric cubic Cu2ZnSnS4 nanoparticles. Chemical Physics Letters, 2014, 608, 393-397.	2.6	17
172	Unravelling the composition of the surface layers formed on Cu, Cu-Ni, Cu-Zn and Cu-Ni-Zn in clean and polluted environments. Applied Surface Science, 2015, 346, 158-164.	6.1	17
173	Dopant-free hole-transporting polymers for efficient, stable, and hysteresis-less perovskite solar cells. Sustainable Materials and Technologies, 2020, 26, e00226.	3.3	17
174	Coaxial nanofibers outperform uniaxial nanofibers for the loading and release of pyrroloquinoline quinone (PQQ) for biomedical applications. Nanoscale Advances, 2020, 2, 3341-3349.	4.6	17
175	Interplay of quantum capacitance with Van der Waals forces, intercalation, co-intercalation, and the number of MoS2 layers. Materials Today Energy, 2021, 20, 100677.	4.7	17
176	Cylindrical C ₉₆ Fullertubes: A Highly Active Metalâ€Free O ₂ â€Reduction Electrocatalyst. Angewandte Chemie - International Edition, 2022, 61, .	13.8	17
177	Potential of 5-methyl 1-H benzotriazole to suppress the dissolution of $\hat{1}$ -aluminum bronze in sulfide-polluted salt water. Materials Chemistry and Physics, 2014, 144, 55-65.	4.0	16
178	Influence of substrate temperature on the properties of electrodeposited kesterite Cu2ZnSnS4 (CZTS) thin films for photovoltaic applications. Journal of Materials Science: Materials in Electronics, 2015, 26, 222-228.	2.2	16
179	DFT insights into the electronic and optical properties of fluorine-doped monoclinic niobium pentoxide (B-Nb2O5:F). Applied Physics A: Materials Science and Processing, 2016, 122, 1.	2.3	16
180	Defect states determined the performance of dopant-free anatase nanocrystals in solar fuel cells. Solar Energy, 2017, 144, 445-452.	6.1	16

#	Article	IF	CITATIONS
181	Multiple synergistic effects of Zr-alloying on the phase stability and photostability of black niobium oxide nanotubes as efficient photoelectrodes for solar hydrogen production. Applied Catalysis B: Environmental, 2021, 287, 119961.	20.2	16
182	Leakage current reduction in n-GaN/p-Si (100) heterojunction solar cells. Applied Physics Letters, 2021, 118, .	3.3	16
183	Surface engineering of nanotubular ferric oxyhydroxide "goethite―on platinum anodes for durable formic acid fuel cells. International Journal of Hydrogen Energy, 2021, , .	7.1	16
184	Symmetric supercapacitor devices based on pristine g-C3N4 mesoporous nanosheets with exceptional stability and wide operating voltage window. Journal of Energy Storage, 2022, 52, 104850.	8.1	16
185	Electrochemical and stress corrosion cracking behavior of 67Cu–33Zn alloy in aqueous electrolytes containing chloride and nitrite ions: Effect of di-sodium hydrogen phosphate (DSHP). Materials Science and Engineering B: Solid-State Materials for Advanced Technology, 2009, 156, 84-89.	3.5	15
186	Effect of Substrate on the Photodetection Characteristics of ZnO-PAni Composites. ECS Journal of Solid State Science and Technology, 2016, 5, P305-P308.	1.8	15
187	Large-diameter light-scattering complex multipodal nanotubes with graded refractive index: insights into their formation mechanism and photoelectrochemical performance. Journal of Materials Chemistry A, 2017, 5, 23600-23611.	10.3	15
188	Silkworms as a factory of functional wearable energy storage fabrics. Scientific Reports, 2019, 9, 12649.	3.3	15
189	Fullerene C ₇₆ as a novel electrocatalyst for VO ²⁺ /VO ₂ ⁺ and chlorine evolution inhibitor in all-vanadium redox flow batteries. Chemical Communications, 2020, 56, 7569-7572.	4.1	15
190	Intranasal lipid nanocapsules for systemic delivery of nimodipine into the brain: In vitro optimization and in vivo pharmacokinetic study. Materials Science and Engineering C, 2020, 116, 111236.	7.3	15
191	An innovative electrochemical platform for the sensitive determination of the hepatitis B inhibitor Entecavir with ionic liquid as a mediator. Journal of Molecular Liquids, 2020, 302, 112498.	4.9	15
192	Ethanol vapor processing of titania nanotube array films: enhanced crystallization and photoelectrochemical performance. Journal of Materials Chemistry, 2009, 19, 3895.	6.7	14
193	Enhanced light sensing characteristics of nanostructured gallium nitride/silicon heterojunctions: Interface matters. Journal of Applied Physics, 2013, 114, .	2.5	14
194	Design and synthesis of new Ru-complexes as potential photo-sensitizers: experimental and TD-DFT insights. RSC Advances, 2016, 6, 69647-69657.	3.6	14
195	Bifunctional Tailoring of Platinum Surfaces with Earth Abundant Iron Oxide Nanowires for Boosted Formic Acid Electro-Oxidation. Journal of Nanotechnology, 2018, 2018, 1-10.	3.4	14
196	Low-temperature thermoelectric performance of novel polyaniline/iron oxide composites with superior Seebeck coefficient. Applied Physics A: Materials Science and Processing, 2019, 125, 1.	2.3	14
197	Comparison between hydrogen production via H2S and H2O splitting on transition metal-doped TiO2 (101) surfaces as potential photoelectrodes. International Journal of Hydrogen Energy, 2020, 45, 26758-26769.	7.1	14
198	Rb intercalation enhanced the supercapacitive performance of layer-structured MoS ₂ as a 2D model material. Materials Advances, 2021, 2, 5052-5056.	5.4	14

#	Article	IF	CITATIONS
199	Ternary Ti–Mo–Fe Nanotubes as Efficient Photoanodes for Solar-Assisted Water Splitting. Journal of Physical Chemistry C, 2021, 125, 12504-12517.	3.1	14
200	Analytical modeling of the radial pn junction nanowire solar cells. Journal of Applied Physics, 2014, 116, .	2.5	13
201	Influence of electrolyte composition on the formation of mixed oxide nanotube arrays for solar fuel production. Journal of Power Sources, 2015, 280, 339-346.	7.8	13
202	Defect engineering in 1D Ti–W oxide nanotube arrays and their correlated photoelectrochemical performance. Physical Chemistry Chemical Physics, 2018, 20, 10258-10265.	2.8	13
203	Refractory plasmonics: orientation-dependent plasmonic coupling in TiN and ZrN nanocubes. Physical Chemistry Chemical Physics, 2018, 20, 1881-1888.	2.8	13
204	Front dielectric and back plasmonic wire grating for efficient light trapping in perovskite solar cells. Optical Materials, 2018, 86, 311-317.	3.6	13
205	Correlation between microstructural defects and photoelectrochemical performance of 1D Ti–Nb composite oxide photoanodes for solar water splitting. International Journal of Hydrogen Energy, 2019, 44, 24418-24429.	7.1	13
206	First-principles descriptors of CO chemisorption on Ni and Cu surfaces. Physical Chemistry Chemical Physics, 2019, 21, 11476-11487.	2.8	13
207	Oxygen Vacancyâ€Engineered Tiâ^'Moâ^'Ni Ternary Oxide Nanotubes as Binderâ€Free Supercapacitor Electrodes with Exceptional Potential Window. ChemNanoMat, 2020, 6, 1513-1518.	2.8	13
208	FeMoO4 nanoparticles as functional negative electrode material for high performance supercapacitor devices over a wide pH range. Journal of Energy Storage, 2022, 54, 105272.	8.1	13
209	Recent advances in the use of density functional theory to design efficient solar energy-based renewable systems. Journal of Renewable and Sustainable Energy, 2013, 5, .	2.0	12
210	Broadband Absorption Enhancement in Thin Film Solar Cells Using Asymmetric Double-Sided Pyramid Gratings. Journal of Electronic Materials, 2016, 45, 5685-5694.	2.2	12
211	Photoactive catalysts for effective water microbial purification: Morphology-activity relationship. Environmental Nanotechnology, Monitoring and Management, 2018, 10, 87-93.	2.9	12
212	Toward the Proper Selection of Carbon Electrode Materials for Energy Storage Applications: Experimental and Theoretical Insights. Energy & Fuels, 2021, 35, 13426-13437.	5.1	12
213	Deciphering the <i>In Situ</i> Surface Reconstruction of Supercapacitive Bimetallic Ni-Co Oxyphosphide during Electrochemical Activation Using Multivariate Statistical Analyses. ACS Applied Energy Materials, 2022, 5, 7661-7673.	5.1	12
214	Electrochemical and Stress Corrosion Cracking Behavior of α-Aluminum Bronze and α-Brass in Nitrite Solutions: A Comparative Study. Corrosion, 2013, 69, 77-84.	1.1	11
215	Single-Crystal Electrospun Plasmonic Perovskite Nanofibers. Journal of Physical Chemistry C, 2018, 122, 6846-6851.	3.1	11
216	Boosting the cyclic stability and supercapacitive performance of graphene hydrogels via excessive nitrogen doping: Experimental and DFT insights. Sustainable Materials and Technologies, 2020, 25, e00206.	3.3	11

#	Article	IF	CITATIONS
217	Structural engineering of Ti-Mn bimetallic phosphide nanotubes for efficient photoelectrochemical water splitting. International Journal of Hydrogen Energy, 2021, 46, 3605-3614.	7.1	11
218	Highly porous Ba3Ti4Nb4O21 perovskite nanofibers as photoanodes for quasi-solid state dye-sensitized solar cells. Solar Energy, 2020, 206, 413-419.	6.1	10
219	A novel and ultrasensitive electrochemical biosensor based on MnO2-V2O5 nanorods for the detection of the antiplatelet prodrug agent Cilostazol in pharmaceutical formulations. Microchemical Journal, 2021, 164, 105946.	4.5	10
220	Bandgap bowing in Ta-W-O system for efficient solar energy conversion: Insights from density functional theory and X-ray diffraction. Applied Physics Letters, 2013, 103, 133905.	3.3	9
221	Rapid and controlled electrochemical synthesis of crystalline niobium oxide microcones. MRS Communications, 2015, 5, 495-501.	1.8	9
222	Plasmonic scattering nanostructures for efficient light trapping in flat CZTS solar cells. Proceedings of SPIE, 2017, , .	0.8	9
223	Photophysical performance of radio frequency sputtered Pt/n-PSi/ZnO NCs/Pt photovoltaic photodetectors. Optical Materials, 2018, 84, 830-842.	3.6	9
224	Experimental and density functional theory insights into the effect of withdrawing ligands on the fluorescence yield of Ru(II)â€based complexes. Applied Organometallic Chemistry, 2019, 33, e4677.	3.5	9
225	Metal-decorated carbon nanotubes-based sensor array for simultaneous detection of toxic gases. Journal of Environmental Chemical Engineering, 2021, 9, 104534.	6.7	9
226	Mapping the stability of free-jet biogas flames under partially premixed combustion. Energy, 2021, 220, 119749.	8.8	9
227	Optical and electronic properties of niobium oxynitrides with various N/O ratios: insights from first-principles calculations. Journal of Photonics for Energy, 2018, 8, 1.	1.3	9
228	Unraveling the structure and electrochemical supercapacitive performance of novel tungsten bronze synthesized by facile template-free hydrothermal method. Electrochimica Acta, 2022, 401, 139494.	5.2	9
229	Adsorption–Desorption Kinetics of Benzotriazole on Cathodically Polarized Copper. Journal of the Electrochemical Society, 2010, 157, C174.	2.9	8
230	Effect of Annealing on the Stress Corrosion Cracking of α-Brass in Aqueous Electrolytes Containing Aggressive Ions. Industrial & Engineering Chemistry Research, 2010, 49, 9529-9533.	3.7	8
231	A facile room temperature electrochemical deposition of pyramidal ZnO nanostructures: Suppressing the green emission. Physica E: Low-Dimensional Systems and Nanostructures, 2012, 44, 1853-1856.	2.7	8
232	Interface architecture determined the performance of ZnO nanorods-based photodetectors. Chemical Physics Letters, 2014, 604, 22-26.	2.6	8
233	Low-Temperature Solution-Processed Flexible Solar Cells Based on (In,Ga)N Nanocubes. ACS Applied Materials & Interfaces, 2014, 6, 9925-9931.	8.0	8
234	Tin oxide as a promoter for copper@palladium nanoparticles on graphene sheets during ethanol electro-oxidation in NaOH solution. Journal of Molecular Liquids, 2020, 297, 111816.	4.9	8

#	Article	IF	CITATIONS
235	Biogas production enhancement using nanocomposites and its combustion characteristics in a concentric flow slot burner. Experimental Thermal and Fluid Science, 2020, 113, 110014.	2.7	8
236	Wellâ€dispersed Au nanoparticles prepared via magnetron sputtering on TiO ₂ nanotubes with unprecedentedly high activity for water splitting. Electrochemical Science Advances, 2021, 1, e2000004.	2.8	8
237	Investigation of the thermal stability of the antihypertensive drug nebivolol under different conditions: Experimental and computational analysis. Journal of Thermal Analysis and Calorimetry, 2022, 147, 5779-5786.	3.6	8
238	Sensitive Determination of SARS-COV-2 and the Anti-hepatitis C Virus Agent Velpatasvir Enabled by Novel Metal–Organic Frameworks. ACS Omega, 2021, 6, 26791-26798.	3.5	8
239	Optimized Lithography-Free Fabrication of Sub-100 nm Nb ₂ O ₅ Nanotube Films as Negative Supercapacitor Electrodes: Tuned Oxygen Vacancies and Cationic Intercalation. ACS Applied Materials & Interfaces, 2022, 14, 25545-25555.	8.0	8
240	ZnO Nanorods/Polyaniline-Based Inorganic/Organic Heterojunctions for Enhanced Light Sensing Applications. ECS Journal of Solid State Science and Technology, 2016, 5, P142-P147.	1.8	7
241	High-performance nanoporous silicon-based photodetectors. Optik, 2018, 168, 424-431.	2.9	7
242	Position of the anchoring group determined the sensitization efficiency of metal-free D-ï€-A dyes: Combined experimental and TD–DFT insights. Journal of Photochemistry and Photobiology A: Chemistry, 2018, 367, 128-136.	3.9	7
243	Electrochemical Fabrication of Ternary Black Tiâ€Moâ€Ni Oxide Nanotube Arrays for Enhanced Photoelectrochemical Water Oxidation. ChemistrySelect, 2020, 5, 12151-12158.	1.5	7
244	Temperature-dependent transport properties of CVD-fabricated n-GaN nanorods/p-Si heterojunction devices. RSC Advances, 2020, 10, 33526-33533.	3.6	7
245	"Salt-in-Fiber―Electrolyte Enables High-Voltage Solid-State Supercapacitors. ACS Applied Energy Materials, 2022, 5, 6410-6416.	5.1	7
246	Electrochemical characterization and stress corrosion cracking behavior of \hat{I}_{\pm} -brass in molybdate-containing electrolytes. Journal of Solid State Electrochemistry, 2012, 16, 353-360.	2.5	6
247	Aqueous synthesis of visible-light photoactive cuboid Cu2ZnSnS4 nanocrystals using rotary evaporation. Materials Letters, 2014, 125, 195-197.	2.6	6
248	Ni-free, built-in nanotubular drug eluting stents: Experimental and theoretical insights. Materials Science and Engineering C, 2019, 103, 109750.	7.3	6
249	Synthesis of Selfâ€Ordered Tantalumâ€Niobium Mixed Oxide Nanotubes and Their Use for Clean Hydrogen Production. ChemNanoMat, 2020, 6, 1617-1619.	2.8	6
250	Anionic/nonionic surfactants for controlled synthesis of highly concentrated sub-50 nm polystyrene spheres. Nanoscale Advances, 2021, 3, 5626-5635.	4.6	6
251	Tailor-designed nanowire-structured iron and nickel oxides on platinum catalyst for formic acid electro-oxidation. RSC Advances, 2022, 12, 20395-20402.	3.6	6
252	Unveiling the role of carbon defects in the exceptional narrowing of m-ZrO2 wide-bandgap for enhanced photoelectrochemical water splitting. International Journal of Hydrogen Energy, 2021, 46, 21499-21511.	7.1	5

#	Article	IF	CITATIONS
253	Growth of high-quality GaN nanowires on p-Si (1 1 1) and their performance in solid state heterojunction solar cells. Solar Energy, 2021, 227, 525-531.	6.1	5
254	Maximizing the electronic charge carriers in donor-doped hematite under oxygen-rich conditions via doping and co-doping strategies revealed by density functional theory calculations. Journal of Applied Physics, 2022, 131, 155705.	2.5	5
255	An alternative, low-dissolution counter electrode to prevent deceptive enhancement of HER overpotential. Scientific Reports, 2022, 12, .	3.3	5
256	Recent Advances in the Use of Silicon-Based Photocathodes for Solar Fuel Production. , 2018, , 229-267.		4
257	Computational Modeling for Biomimetic Sensors. Methods in Molecular Biology, 2019, 2027, 195-210.	0.9	4
258	Synergistic effect of silver and adenine on boosting the supercapacitance performance of spongy graphene. Journal of Energy Storage, 2019, 24, 100776.	8.1	4
259	Efficient dye-sensitized solar cells based on bioinspired copper redox mediators by tailoring counterions. Journal of Materials Chemistry A, 2022, 10, 4131-4136.	10.3	4
260	Untapped potential of 2D charge density wave chalcogenides as negative supercapacitor electrode materials. RSC Advances, 2022, 12, 6433-6439.	3.6	4
261	Black silicon based on simple fabrication of mesoporous silicon nanowires for solar energy harvesting. , 2016, , .		3
262	Facile omnidirectional black silicon based on porous and nonporous silicon nanowires for energy applications. , 2016, , .		3
263	Numerical simulation and a parametric study of inorganic nanowire solar cells. International Journal of Numerical Modelling: Electronic Networks, Devices and Fields, 2017, 30, e2176.	1.9	3
264	A facile synthesis of zeolitic analcime/spongy graphene nanocomposites as novel hybrid electrodes for symmetric supercapacitors. Journal of Energy Storage, 2020, 32, 101953.	8.1	3
265	Photoelectrocatalytic hydrogen production on ternary Coâ€Pi /Ag/ TiON nanotube array photocatalysts. International Journal of Energy Research, 2021, 45, 6360-6368.	4.5	3
266	Cylindrical C ₉₆ Fullertubes: A Highly Active Metalâ€Free O ₂ â€Reduction Electrocatalyst. Angewandte Chemie, 0, , .	2.0	3
267	Deciphering the hype effect of Ni-foam substrate in electrochemical supercapacitors: Is there a way out?. Materials Today Communications, 2022, 32, 103972.	1.9	3
268	Laser annealing enhanced the photophysical performance of Pt/n-PSi/ZnO/Pt-based photodetectors. Solid-State Electronics, 2020, 171, 107821.	1.4	2
269	Hydrogenated Zinc Oxide as an Alternative Low-Loss Plasmonic Material with Fano Resonance in Near-IR. Journal of Physical Chemistry C, 2022, 126, 8190-8198.	3.1	2
270	Towards a perfect system for solar hydrogen production: an example of synergy on the atomic scale. , 2013, , .		1

#	Article	IF	CITATIONS
271	Nanotubes: An Experimental Insight into the Structural and Electronic Characteristics of Strontium-Doped Titanium Dioxide Nanotube Arrays (Adv. Funct. Mater. 43/2014). Advanced Functional Materials, 2014, 24, 6782-6782.	14.9	1
272	Silicon Nanowires with controlled diameter for energy conversion applications. , 2013, , .		1
273	Simple scalable fabrication method of wide-angle black silicon surface for energy-harvesting applications. , 2018, , .		1
274	Anodically Fabricated Sr-doped TiO2 Nanotube Arrays for Photoelectrochemical Water Splitting Applications. Materials Research Society Symposia Proceedings, 2011, 1352, 151.	0.1	0
275	D7. Fabrication of crystalline silicon nanowires with different dimensions for solar cell applications. , 2015, , .		Ο
276	Optimization of the fabricated silicon nanowires for energy-harvesting applications. Proceedings of SPIE, 2015, , .	0.8	0
277	Optimizing absorption and scattering cross section of metal nanostructures for enhancing light coupling inside perovskite solar cells. , 2017, , .		Ο
278	Photophysical performance of Nd-YAG annealed Pt/n-PSi /Pt photovoltaic photodetectors at different laser energy. Optical and Quantum Electronics, 2020, 52, 1.	3.3	0
279	Novel silicon bipodal cylinders with controlled resonances and their use as beam steering metasurfaces. Scientific Reports, 2021, 11, 13635.	3.3	Ο
280	All dielectric and plasmonic cross-grating metasurface for efficient perovskite solar cells. , 2018, , .		0
281	Plasmonic nanoscatter antireflective coating for efficient CZTS solar cells. , 2018, , .		Ο
282	Using all dielectric and plasmonic cross grating metasurface for enhancing efficiency of CZTS solar cells. , 2018, , .		0
283	Design of optimum back contact plasmonic nanostructures for enhancing light coupling in CZTS solar cells. , 2018, , .		Ο
284	Enhancing light absorption inside CZTS solar cells using plasmonic and dielectric wire grating metasurface. , 2018, , .		0
285	Design methodology for selecting optimum plasmonic scattering nanostructures inside CZTS solar cells. , 2018, , .		0
286	Towards accurate ionic relaxation algorithms for two-dimensional chalcogenide van der Waals materials - A first-principles study. Physica E: Low-Dimensional Systems and Nanostructures, 2022, 140, 115223.	2.7	0